Proceedings of IMECE2005
2005 ASME International Mechanical Engineering Congress and Exposition
November 5-11, 2005, Orlando, Florida USA

IMECE2005-82037

ROBUST TIME-OPTIMAL COMMAND SHAPING FOR PIEZOELECTRIC ACTUATORS: STM APPLICATION

Y. Xu
Department of Mechanical Engineering,
Purdue University
West Lafayette, IN 47907, USA
xuy@purdue.edu

P.H. Meckl
Department of Mechanical Engineering,
Purdue University
West Lafayette, IN 47907, USA
meckl@purdue.edu

ABSTRACT

A scanning tunneling microscope (STM) uses a piezo-electric actuator to perform constant-velocity scanning motion. Many feedback strategies have been proposed, but their achievable scan rate is substantially limited by the turnaround transients in the scan path. Therefore, a robust time-optimal command shaping technique with an iterative search procedure is introduced in this paper to improve the scan speed of piezoactuators, and is applicable to a general class of systems without rigid-body mode. Furthermore, a time-energy-optimal formulation is presented to reduce the in-maneuver oscillation. The hysteresis nonlinearity of piezoactuators is compensated using the proposed continuous numerical inversion algorithm. Finally, the closed-loop simulation shows the performance robustness in the presence of hysteresis cancellation error and natural frequency perturbation.

INTRODUCTION

Compared to traditional actuators, piezoelectric actuators (or PZT actuators for short) offer enormous advantages, such as high bandwidth, theoretically unlimited resolution, and no friction or wear. Therefore, they have found wide applications in atomic force microscopes, optical fiber aligners, hard disks, and microelectronics. This paper focuses on the application of PZT actuators to STM (Scanning Tunneling Microscopy) which is a tool to manipulate materials at the atomic level. A typical scanning trajectory of STM consists of a constant-velocity-scan region and a return transition region [1]. Because the probe/actuator system of a STM is inherently flexible, the induced vibration is the major limiting factor in achievable scanning precision and speed.

Many feedback strategies have been proposed to achieve precision scanning maneuvers. Salapaka et al. [2][3] have developed a higher-order controller based on H-infinity techniques for the x-y motion of a piezo stack actuator. Tan and Baras [4] developed a robust control framework for smart actuators by combining inverse control with the l_1 robust control theory. Li et al. [5] presented a learning self-tuning regulator (LSTR) which improves the tracking performance of PZT actuators. Daniele et al. [6] designed a controller using loop shaping technique.

Though the use of feedback control improves linearity, the maximum scan rate is substantially limited by the turnaround transients due to velocity changes in the scan path [7]. Therefore, a feedforward approach is considered here to address the speed problem of STM. Devasia and his co-workers [1][7][8] proposed a feedforward approach that integrates standard optimal control techniques with the model-based inversion method to solve the optimal scanning problem. Xu and Meckl [15] developed a time-optimal command shaping scheme based on a constrained least-square method that pushes the scanning rate beyond the first resonant frequency.

Other major concerns in STM application are hysteresis and creep nonlinearities inherent to the piezoelectric actuator. Since creep (or drift) changes very slowly, it can be easily corrected using a feedback controller. On the other hand, hysteresis is more significant and needs to be explicitly modeled and compensated. There are many ways to model hysteresis, e.g., polynomial models, neural networks, and Maxwell's model. In the past few years, the classical Preisach model and its derivatives [9][10] has emerged as the preferred model for engineering applications because of its generality and practicality [11].

Many hysteresis inversion methods have been proposed. Hughes and Wen [12] utilized the monotonic nature of the first-order reversal curves to invert the hysteresis function. Venkataraman and Krishnaprasad [13] proposed an inversion algorithm based on the contraction mapping principle by exploiting the properties of Lipschitz continuity and incrementally strict increase of the Preisach operator under some mild assumptions. Tan et al. [14] developed the Closest Match Algorithm for the inversion directly based on a discretized hysteresis model. In an earlier paper of the authors, Xu and Meckl [15] proposed a continuous numerical inversion algorithm (CNIA) that searches for the numerical approximation of the inverse hysteresis.

By compensating hysteresis using the abovementioned CNIA, this paper introduces a robust command shaping technique based on the linear dynamics of the PZT actuator. In particular, robustness to natural frequency errors is desired. An iterative search method is used to obtain the time-optimal solution for velocity tracking, and a time-energy-optimal formulation is presented to reduce in-maneuver oscillation. Finally, the feedforward design is simulated in a closed-loop structure.

MODELING

A PZT actuator can be modeled as the composition of a hysteresis component H and a linear dynamic component G as shown in Fig. 1. Tao and Kokotovic [16] showed that accurate position control is achievable if an inverse operator H^{-1} can be found such that H and H^{-1} "cancel" each other, thus allowing the controller to be designed based on the linear dynamics.

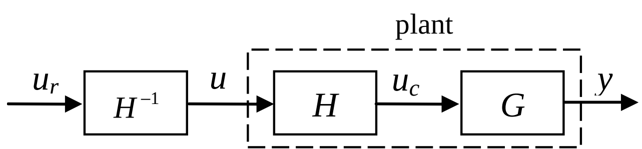

Fig. 1. A PZT actuator model

The linear component G of the PZT actuator model used in this paper is a 4th-order transfer function adopted from [1]. The system parameters are given in Table I.

$$G(s)=\frac{K\left(s^2-2\zeta_z\omega_z s+\omega_z^2\right)}{\left(s^2+2\zeta_1\omega_1 s+\omega_1^2\right)\left(s^2+2\zeta_2\omega_2 s+\omega_2^2\right)} \tag{1}$$

TABLE I
PARAMETERS OF PZT ACTUATOR MODEL

	ζ	$f\,(\mathrm{Hz})$
NMP zero	0.70	1643
First mode	0.008	242
Second mode	0.39	777
K	97000	

HYSTERESIS COMPENSATION

A continuous numerical inversion algorithm (CNIA) based on the classical Preisach Model was proposed in the authors' earlier paper [15]. Instead of trying to find the exact inversion operator, the CNIA searches for the numerical approximation of the inverse hysteresis, thus dramatically reducing the mathematical complexity of the inversion problem.

The CNIA yields a control input u^* such that

$$\left|\hat{\Gamma}(u^*;\psi)-f_d\right|\le\varepsilon, \qquad u^*\in\left[u_{\min},u_{\max}\right] \tag{2}$$

where $\hat{\Gamma}$ is the Preisach operator of the identified hysteresis model, ψ is the input history, f_d is the desired hysteresis output and $\varepsilon>0$ is the allowed approximation error.

As each reversal curve (either ascending or descending) of the hysteresis is monotonic, the proposed search algorithm is guaranteed to converge. The number of iterations needed depends on the choice of the stopping threshold ε.

The simulation result of open-loop hysteresis compensation is shown in Fig. 2. The notation of u_r, u_c in the figures is defined in Fig. 1. The threshold ε is set to 0.2% of the input range in this example. The figure shows that the original hysteresis is almost linearized.

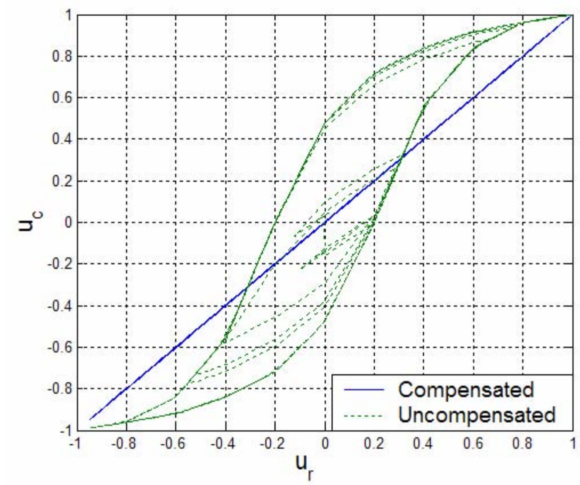

Fig. 2. Linearization of the hysteresis nonlinearity

ROBUST TIME-OPTIMAL COMMAND SHAPING

A. Optimization scheme

The proposed robust time-optimal command shaping is based on the constrained least-square method proposed by Reynolds and Meckl [17]. Given a discrete-time system

$$\begin{aligned}\mathbf{x}(k+1)&=\mathbf{A}\mathbf{x}(k)+\mathbf{B}u(k)\\ y(k)&=\mathbf{C}\mathbf{x}(k)\end{aligned} \tag{3}$$

subject to the tracking constraint and actuator limit

$$\left|y(k)-y_d(k)\right|\le e_{allow}(k) \tag{4}$$

$$\left|u(k)\right|\le F_{\max} \tag{5}$$

By incorporating the constraints (4)(5) at each point on the trajectory in a least-square programming scheme, a time-optimal input profile can be obtained by increasing k until a solution satisfying the constraints results. The optimization problem is formulated as

$$\begin{aligned}&\min\quad \left\{\left(\mathbf{x}(k)-\mathbf{x}_d\right)^T\left(\mathbf{x}(k)-\mathbf{x}_d\right)\right\}^{1/2}\\ &\mathbf{U}(k)\quad \text{subject to (4), (5)}\end{aligned} \tag{6}$$

Many standard packages are available for solving linear least-square programming problems, including MATLAB.

B. Robust command shaping for velocity tracking

Pao and Singhose [18] showed that the robust time-optimal shaper design is equivalent to the traditional time-optimal control problem on an augmented system where the vibrational modes of the original model are purposely repeated. By locating multiple zeros at (or near) the system poles, the input is made less sensitive to model uncertainties.

Input robustness from the zero-placing technique has been mathematically proved by Bhat and Miu [19] from the perspective of frequency domain. Assume an n-dimensional single-input system has been put into the Jordan canonical form as

$$\dot{\mathbf{q}}(t)=\mathbf{J}\mathbf{q}(t)+\mathbf{B}^{*}u(t)=\begin{bmatrix}\mathbf{J}_1 & & \\ & \ddots & \\ & & \mathbf{J}_n\end{bmatrix}\mathbf{q}(t)+\begin{bmatrix}\mathbf{B}_1^{*}\\ \vdots \\ \mathbf{B}_n^{*}\end{bmatrix}u(t) \qquad (7)$$

where

$$\mathbf{J}_i=\begin{pmatrix}p_i & 1 & & \\ & p_i & & \\ & & \ddots & 1\\ & & & p_i\end{pmatrix},\mathbf{B}_i^{*}=\begin{pmatrix}0\\0\\ \vdots\\1\end{pmatrix},\ (i=1,\ldots,n)$$

correspond to a pole p_i with multiplicity m_i. Bhat and Miu showed the sufficient condition for robustness of a time-bounded input as

$$\frac{1}{(m_i-j)!}\frac{d^{m_i-j}}{ds^{m_i-j}}U(s)\Big|_{s=p_i}=\sum_{k=j}^{m_i}\left[q_{ik}(T)\frac{(-T)^{k-j}}{(k-j)!}e^{-p_iT}\right]-q_{ij}(0) \qquad (8)$$

However, for velocity tracking, the input after time T (when the system reaches the desired scanning speed) increases at a constant rate w_{ss} to maintain the constant velocity output and therefore is not time-bounded, as illustrated in Fig. 3. In order to derive the sufficient condition of input robustness for velocity tracking, the input profile in Fig. 3 is divided into two sections: the input history before time T is denoted as $u_T(t)$, and the part after time T as $u_\infty(t)$. The Laplace transform of the input is:

$$U(s)=\int_0^T u_T(t)e^{-st}dt+\int_T^\infty u_\infty(t)e^{-st}dt \qquad (9)$$

By defining

$$U_T(s)=\int_0^T u_T(t)e^{-st}dt \qquad (10)$$

and noting that $u_\infty(t)$ can be approximated by

$$u_\infty(t)=u_T(T)+w_{ss}\left(t-T\right) \qquad (11)$$

(9) becomes

$$U(s)=U_T(s)+\frac{u_T(T)s+w_{ss}}{s^2}e^{-sT} \qquad (12)$$

Since $u_T(t)$ is a time bounded signal, the sufficient condition (8) can be directly applied to it. Therefore we have

$$\frac{1}{(m_i-j)!}\frac{d^{m_i-j}}{ds^{m_i-j}}U_T(s)\Big|_{s=p_i}=\sum_{k=j}^{m_i}\left[q_{ik}(T)\frac{(-T)^{k-j}}{(k-j)!}e^{-p_iT}\right]-q_{ij}(0)$$

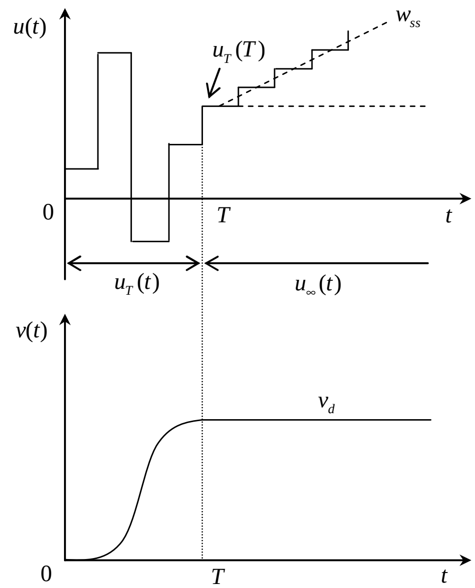

Fig. 3. Input feature of velocity tracking.

Substituting (12) into the above equation, we obtain the sufficient condition in the frequency domain for the robustness of a velocity-tracking input:

$$\begin{aligned}\frac{1}{(m_i-j)!}\frac{d^{m_i-j}}{ds^{m_i-j}}U(s)\Big|_{s=p_i}&=\sum_{k=j}^{m_i}\left[q_{ik}(T)\frac{(-T)^{k-j}}{(k-j)!}e^{-p_iT}\right]\\ &\quad -q_{ij}(0)+\frac{1}{(m_i-j)!}D_{m_i-j}(p_i)\end{aligned} \qquad (13)$$

where

$$D_{m_i-j}(p_i)=\frac{d^{m_i-j}}{ds^{m_i-j}}\left[\frac{u_T(T)s+w_{ss}}{s^2}e^{-sT}\right]_{s=p_i}$$

In the rest of this paper, we call a robust input obtained using the augmented system with multiplicity $m+1$ for a mode as "*m*-th order robust" with respect to that mode.

Suppose a 2nd-order input robustness for the *i*-th mode is desired. The Jordan block corresponding to this mode is augmented to $m_i=3$ as:

$$\begin{bmatrix}\dot q_{i1}\\ \dot q_{i2}\\ \dot q_{i3}\\ \dot q_{i1}^c\\ \dot q_{i2}^c\\ \dot q_{i3}^c\end{bmatrix}=\left[\begin{array}{ccc|ccc}p_i & 1 & & & & \\ & p_i & 1 & & \mathbf{0} & \\ & & p_i & & & \\ \hline & & & p_i^* & 1 & \\ & \mathbf{0} & & & p_i^* & 1\\ & & & & & p_i^*\end{array}\right]\begin{bmatrix}q_{i1}\\ q_{i2}\\ q_{i3}\\ \dot q_{i1}^c\\ \dot q_{i2}^c\\ \dot q_{i3}^c\end{bmatrix}+\begin{bmatrix}0\\0\\1\\0\\0\\1\end{bmatrix}u \qquad (14.1)$$

The corresponding block in the output matrix is augmented as

$$\mathbf{C}_i=\begin{bmatrix}0 & 0 & c_i & 0 & 0 & c_i^*\end{bmatrix} \qquad (14.2)$$

Here we only discuss for the pole p. The case for the other pole p^* can be easily developed in the same manner. Assuming zero initial conditions in (13), we have:

(a) $j = 3 \Rightarrow m_i - j = 0$:

To have $U(s)|_{s=p_i} = 0$, we set

$$q_{i3}(T) = -\frac{u_T(T)}{p_i} - \frac{w_{ss}}{p_i^2} \tag{15.1}$$

(b) $j = 2 \Rightarrow m_i - j = 1$:

$$\frac{d}{ds}U(s)|_{s=p_i} = \left[q_{i2}(T) - \frac{u_T(T)}{p_i^2} - \frac{2w_{ss}}{p_i^3}\right]e^{-p_iT}$$

To have $\frac{d}{ds}U(s)|_{s=p_i} = 0$, we set

$$q_{i2}(T) = \frac{u_T(T)}{p_i^2} + \frac{2w_{ss}}{p_i^3} \tag{15.2}$$

(c) $j = 1 \Rightarrow m_i - j = 2$:

$$\frac{d^2}{ds^2}U(s)|_{s=p_i} = \left[q_{i1}(T) + \frac{u_T(T)}{p_i^3} + \frac{3w_{ss}}{p_i^4}\right]e^{-p_iT}$$

To have $\frac{d^2}{ds^2}U(s)|_{s=p_i} = 0$, we set

$$q_{i1}(T) = -\frac{u_T(T)}{p_i^3} - \frac{3w_{ss}}{p_i^4} \tag{15.3}$$

The results in (a)-(c) can be summarized into the following general conclusion: for 2nd-order robustification, we set

$$\mathbf{q}_i^T(T) = \left[-\frac{u_T(T)}{p_i^3} - \frac{3w_{ss}}{p_i^4} \quad \frac{u_T(T)}{p_i^2} + \frac{2w_{ss}}{p_i^3} \quad -\frac{u_T(T)}{p_i} - \frac{w_{ss}}{p_i^2}\right] \tag{16}$$

Similarly, for 1st-order robustification, we set

$$\mathbf{q}_i^T(T) = \left[\frac{u_T(T)}{p_i^2} + \frac{2w_{ss}}{p_i^3} \quad -\frac{u_T(T)}{p_i} - \frac{w_{ss}}{p_i^2}\right] \tag{17}$$

The last two equations imply that the choice of the final states $\mathbf{q}_i(T)$ depends on $u_T(T)$ which is supposed to be the result of the optimization. Apparently, the robust command shaping for velocity tracking has two intertwined parts whose solutions depend on each other.

For the PZT actuator model, when substituting (16) into the output matrix of the augmented system, we have

$$y(T) = G(0)u_T(T) + \frac{\beta_y}{G(0)}v_d, \qquad v(T) = v_d \tag{18}$$

where β_y is a constant. The equation (18) indicates that, with the augmented states set as (16), the system will reach the desired speed at the position $y(T)$ whose value is a function of $u_T(T)$. Since $u_T(T)$ is unknown, it means that the system can reach the desired speed at many possible positions. However, we do know that there must be one and only one value of $y(T)$ that gives a minimum-time maneuver.

Therefore, the solution we propose is to iteratively search for the optimal $u_T(T)$ (or equivalently, $y(T)$) that gives the minimum-time maneuver. For each possible value of $y(T)$, the robust command shaping is performed and the maneuver time associated with this $y(T)$ is obtained. By comparing the maneuver times over a range of $y(T)$, the one with the fastest operation is chosen, and the associated input is time-optimal in a robust sense.

In simulation, the scan distance is set to 6 μm, the desired speed $v_d = 10^3$ μm/s, and the velocity tracking tolerance is 0.1 μm/s. The sampling time is 0.2 ms. To test robustness, +10% frequency perturbation is used. Fig. 4 shows the search for the time-optimal solution of the 1st-order robust command shaping, and Fig. 5 shows the input/output profile. In the figure, e_m represents the maximum tracking error due to the plant perturbation, and e_r is the maximum residual vibration due to the plant perturbation. For short, we call e_m the perturbed tracking error, and e_r the perturbed residual vibration.

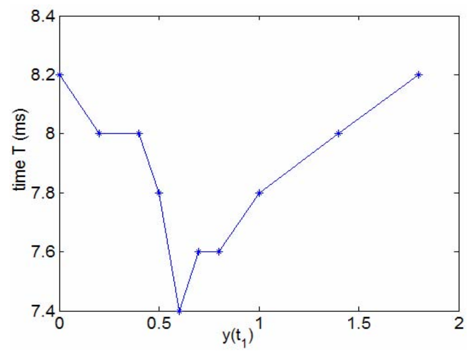

Fig. 4. Time-optimality search for the 1st-order robustness

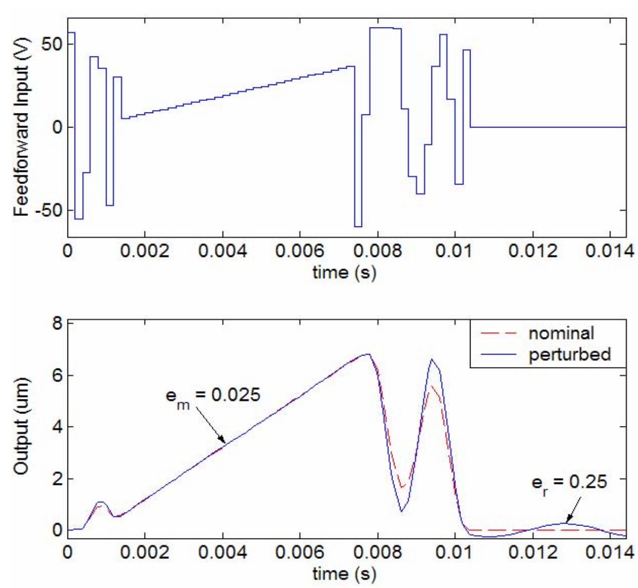

Fig. 5. 1st-order robust input/output of the PZT actuator

To further reduce the perturbed errors e_m and e_r, 2nd-order robust command shaping can be performed. However, increasing the order of robustness slows down the maneuver.

Realizing that for the 1st-order robust input, e_m is good whereas e_r is relatively large, we can adopt a combined-robust input profile to reduce e_r only – the tracking section uses 1st-order robustness, and the return section uses 2nd-order robustness, as shown in Fig. 6. The performances of different inputs are compared in Table II.

TABLE II
PERFORMANCE COMPARISON OF DIFFERENT INPUTS

Input	Cycle time (ms)	e_m (μm)	e_r (μm)
Non-robust	8.4	0.18	1.37
1st-order robust	10.4	0.025	0.25
2nd-order robust	14.8	0.006	0.04
Combined-robust	13.4	0.025	0.04

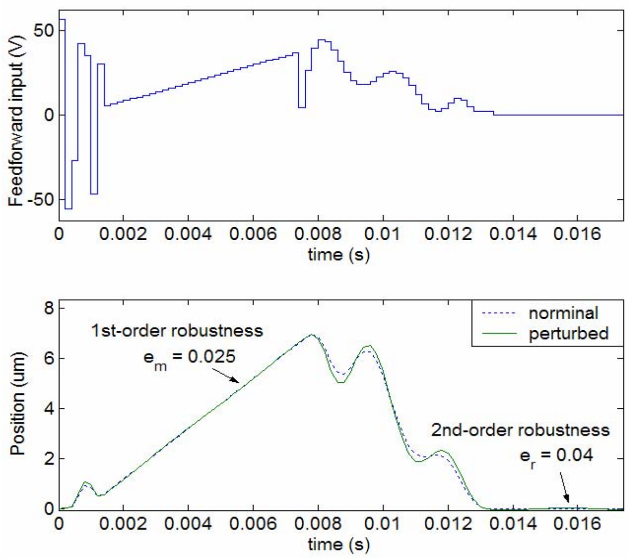

Fig. 6. Combined-robust input/output of the PZT actuator

C. In-maneuver oscillation reduction by energy optimization

In Fig. 5, a remarkable oscillation is observed in the return transition. The large in-maneuver oscillation occurs because the scheme seeks the time-optimal solution. The resulting input is such that the system is driven hard to move quickly, yet at the end of the motion the energy of the excited oscillation is released to achieve zero residual vibration. For this reason, it can be expected that, if the time optimality requirement is relaxed and meanwhile the energy optimal solution is sought, the resulting robust input will be much smoother. A new optimization problem is formulated as

$$J = \min_{\mathbf{U}} \ \frac{1}{2}\mathbf{U}^T\mathbf{U}$$
$$\text{subject to} \begin{cases} \text{(a) } \mathbf{\Phi U} = \mathbf{x}_d - \mathbf{A}^k\mathbf{x}_0 \\ \text{(b) actuator limit (5)} \\ \text{(c) tracking constraint (4) if applicable} \end{cases} \tag{19}$$

where constraint (a) is applied in order to satisfy the set-point requirement and achieve zero residual vibration. Fig. 7 shows a series of 1st-order robust outputs obtained by relaxing the time optimality to different extent. k_r is the number of steps of the return maneuver. With the new formulation, we can trade off between the response speed and transition smoothness.

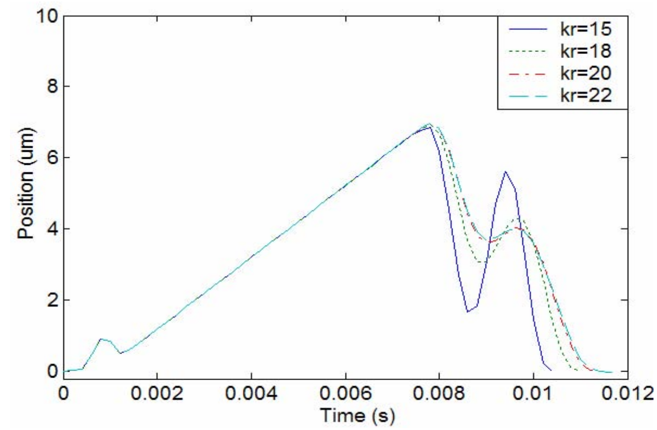

Fig.7. 1st-order robust output with return transition optimization

CLOSED-LOOP IMPLEMENTATION

Although the time-optimal command is an open-loop signal, it can be easily incorporated into a closed-loop framework together with the hysteresis compensation, as illustrated in Fig. 8.

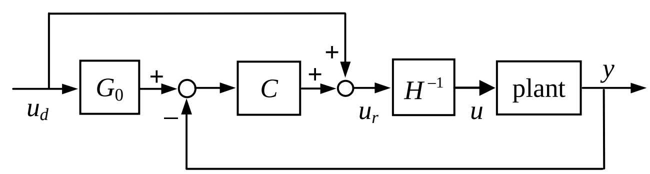

Fig. 8. Closed-loop implementation framework

The feedback controller is designed using pole-placement technique to eliminate creep nonlinearity of the PZT actuator and provide additional robustness for unmodeled dynamics, hysteresis cancellation error, disturbances, and computational delay in digital implementation. Fig. 9 shows the result of the

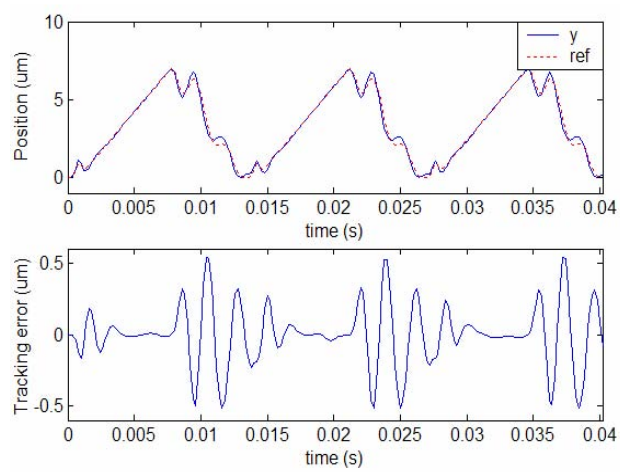

Fig. 9. Closed-loop simulation of the combined-robust input

closed-loop simulation. The frequency perturbation is set to 10%, and the hysteresis cancellation error is 0.15 V. Note that the large tracking error occurs in the transition regions, which we don't care. The tracking error in the active scanning region is $0.07\,\mu m$.

CONCLUSION

Based on the sufficient condition of input robustness in the frequency domain, this paper introduces a robust time-optimal command shaping technique for piezoelectric actuator application in scanning tunneling microscopy to improve the scan speed. This method is general to any system without rigid-body mode. With the proposed continuous numerical inversion algorithm (CNIA), the hysteretic nonlinearity is greatly reduced. In the specific case of a STM where velocity tracking is demanded, an iterative search procedure for the time-optimal solution is proposed. A time-energy-optimal formulation is presented in order to reduce the in-maneuver oscillation. Both open-loop and closed-loop simulations show that the proposed command shaping method generates robust inputs for STM scanning.

REFERENCES

[1] H. Perez, Q. Zou, and S. Devasia, "Design and control of optimal feedforward trajectories for scanners: STM example," *Proceedings of the American Control Conference*, May 2002, pp. 2305-2312.

[2] S. Salapaka, et al., "Design, identification and control of a fast nanopositioning device," *Proceedings of the American Control Conference*, May 2002, pp. 1966-1971.

[3] S. Salapaka, et al., "High bandwidth nano-positioner: A robust control approach," *Review of Scientific Instruments*, Vol. 73, No. 9, Sept. 2002, pp. 3232-3241.

[4] X. Tan, and J. S. Baras, "A robust control framework for smart actuators," *Proceedings of the American Control Conference*, June 2003, pp. 4645-4650.

[5] C. J. Li, et al., "Nonlinear piezo-actuator control by learning self-tuning regulator," *ASME Journal of Dynamic Systems, Measurement, and Control*, Vol. 115, December 1993, pp. 720-723.

[6] A. Daniele, et al, "Piezoelectric scanners for Atomic Force Microscopes: design of lateral sensors, identification and control," *Proceedings of the American Control Conference*, June 1999, pp. 253-257.

[7] D. Croft, and S. Devasia, "Vibration compensation for high speed scanning tunneling microscopy," *Review of Scientific Instruments*, Vol. 70, No. 12, December 1999, pp. 4600-4605.

[8] D. Croft, G. Shedd, and S. Devasia, "Creep, hysteresis, and vibration compensation for piezo-actuators: atomic force microscopy application," *Proceedings of the American Control Conference*, June 2000, pp. 2123-2128.

[9] I.D. Mayergoyz. *Mathematical Models of Hysteresis*. Springer-Verlag, New York, 1991.

[10] I.D. Mayergoyz, and G. Friedman, "Generalized Preisach model of hysteresis," *IEEE Transactions on Magnetics*, Vol. 24, No. 1, Jan. 1988, pp. 212-217.

[11] R.B. Gorbet, "Control of hysteretic systems with Preisach representations," Ph.D. thesis, 1997, University of Waterloo, Canada.

[12] D. Hughes, and J.T. Wen, "Preisach modeling and compensation for smart material hysteresis," in *Active Materials and Smart Structures, Proceedings of SPIE*, Vol. 2427, 1994, pp. 50-64.

[13] R. Venkataraman, P.S. Krishnaprasad, "Approximate inversion of hysteresis: theory and numerical results," *Proceedings of the 39th IEEE Conference on Decision and Control*, Dec. 2000, pp. 4448-4454.

[14] X. Tan, R. Venkataraman, and P.S. Krishnaprasad, "Control of hysteresis: theory and experimental results," in *Modeling, Signal Processing, and Control in Smart Structures, Proceedings of SPIE*, Vol. 4326, 2001, pp. 101-112.

[15] Y. Xu, and P. H. Meckl, "Time-optimal motion control of piezoelectric actuator: STM application," *Proceedings of the American Control Conference*, June 2004, pp. 4849-4854.

[16] G. Tao, and P.V. Kokotovic. *Adaptive control of systems with actuator and sensor nonlinearities*. Wiley, 1996.

[17] M.C. Reynolds, and P. Meckl, "The application of command shaping to the tracking problem," *Proceedings of the American Control Conference*, June 2003, pp. 3148-3153.

[18] L.Y. Pao, and W.E. Singhose, "On the equivalence of minimum time input shaping with traditional time-optimal control," *Proceedings of the IEEE Conference on Control Applications*, Sept. 1995, pp. 1120-1125.

[19] S.P. Bhat, D.K. Miu, "Precise point-to-point positioning control of flexible structures," *ASME Journal of Dynamic Systems, Measurement, and Control*, Vol. 112, December 1990, pp. 667-674.